10.1109/ULTSYM.2015.0439

SPARSE DECONVOLUTION OF ULTRASOUND NDE ECHOES ACCOUNTING FOR PULSE VARIANCE

Ramazan Demirli[1], Juan Lu[2], Pramod Govindan[2], Jafar Saniie[2]*
{ramazan.demirli@villanova.edu, sansonic@ece.iit.edu}

[1]Center for Advanced Communications, Villanova University, Villanova, PA USA
[2] Department of Electrical and Computer Engineering, Illinois Institute of Technology, Chicago, IL USA

***Abstract* — In this paper, we propose a new method of the material reflectivity function (MRF) recovery based on an RF measurement model in which the ultrasound signal is expressed as a sequence of parametric model echoes whose shapes are allowed to vary in accordance with the spectral characteristics of the measuring transducer. We then utilize the Model Based Estimation Pursuit (MBEP) to concurrently estimate the reflectivity and spectral parameters of the echo from the local data. We tested MBEP in comparison with a sparse deconvolution method, the *ℓ1*-regularized Least Squares Deconvolution (*ℓ1-LSD*) via a series of simulated RF data containing varying pulses. The restored MRFs are compared against the ground truths using the correlation match index (CMI) metric. MBEP not only provides more accurate recovery of MRFs but also reveals the frequency dependent attenuation as evident in the pulse spectrum. The *ℓ1-LSD,* however, due to its inflexibility with varying pulses, fails to recover the true scatterers. Further, compared to *ℓ1-LSD,* the MBEP provides about 25% improvement in CMI and is about 10 times computationally faster.**

Index Terms - *Resolution improvement, sparse deconvolution, model based estimation pursuit, MAP estimation.*

I. INTRODUCTION

In ultrasonic nondestructive evaluation (NDE) applications, the backscattered RF signal has information about the geometric shape, size, and orientation of the scatterers within the propagation path. Recently, there has been significant analytical and experimental studies to model the backscattered ultrasonic signal for material characterizations [1-4]. The RF signals obtained by scanning the materials are inherently low-resolution due to the bandlimited nature of the interrogating ultrasound pulse. Such low resolution compromises the quality of information regarding the internal structures of the material. The commonly used approach for improving the resolution of RF data is classical deconvolution techniques such as Wiener filtering. These techniques are sensitive to noise and provide only moderate resolution improvements [1, 2]. More recently, sparse deconvolution techniques have emerged in the field of compressive sensing. These techniques achieve significant resolution gains by exploiting the sparsity of the MRF and show superior performance compared to inversion based methods. Although they are very effective in recovering the MRF when the ultrasound pulse is invariant across the propagation distance, their performance deteriorate when the pulse varies with propagation. To overcome this limitation, they must utilize a realistic model of pulse variance across the material [5].

In this paper, a novel restoration technique, Model Based Estimation Pursuit (MBEP) [6], is used to reconstruct the RF traces in terms of model echoes. MBEP is highly adaptive to the varying pulse without utilizing a learned pulse variance model. This technique has been successfully applied in analyzing microstructure echoes in metals and reverberation echoes from layered media [6], [7].

In our approach, we represent the RF data as superposition of parametric model echoes. The arrival time and amplitude of each model echo represent the local reflectivity while its spectral parameters (bandwidth, center frequency, and phase) represent the locally varying pulse. Maximum a Posteriori (MAP) estimation is utilized to estimate the spectral parameters within user defined limits which in effect controls the pulse variance. The performance of the MBEP algorithm is tested with many realizations of RF data simulated for varying pulse shapes and randomly generated MRFs.

The remainder of the paper is organized as follows. Section 2 introduces the RF measurement model with varying pulse and formulates the MRF estimation. The discussion reviews a sparse deconvolution method (*ℓ1-LSD*) for invariant pulse and introduces the MBEP technique to account for varying pulse. Section 3 presents deconvolution analysis of the simulated RF data for various conditions using MBEP and *ℓ1-LSD* techniques. Section 4 concludes this paper.

II. RF DATA MODEL & SPARSE DECONVOLUTION

We represent an RF line obtained from material by a linear combination of a number of resolvable echoes situated along the transducers focused beam as:

$$y(t_n) = \sum_{m=1}^{M} \beta_m h_m(t_n - \tau_m) + w(t_n), \qquad n = 0,1,...N-1, \qquad (1)$$

where the parameter pairs $\{\tau_m, \beta_m\}$ represent the reflectivity function of the m-th scatterer, and $h_m(t-\tau_m)$ represents the pulse at τ_m. The term $w(t)$ is the measurement noise and characterized as zero-mean white Gaussian noise (WGN) with variance σ_w^2. The ultimate objective of an NDE system is to recover the MRF, i.e., $x = \{\tau_m, \beta_m; m = 1,2,...M\}$ from the measured RF data. Under pulse invariance assumption, i.e., $h_m(t-\tau_m) = h(t-\tau_m)$, the model in (1) can be simplified to,

$$\mathbf{y} = \mathbf{H}\mathbf{x} + \mathbf{w} \qquad (2)$$

where $\mathbf{H}$ represents the convolution matrix of size N x N (whose columns are circularly shifted copies of the transducer pulse $\mathbf{h}$), and $\mathbf{x}$, $\mathbf{w}$, and $\mathbf{y}$ are vectors of length N that represent respectively the MRF, noise, and measured data. If no assumption is made on the characteristics of the MRF $\mathbf{x}$, one obtains the most general pseudo-inverse solution via Least Squares estimation: $\hat{\mathbf{x}} = (\mathbf{H}^T\mathbf{H})^{-1}\mathbf{H}^T\mathbf{y}$. Due to the bandlimited ultrasound pulse $\mathbf{h}$, such a solution is highly sensitive to noise [1]. One can assume a particular priori distribution on $\mathbf{x}$ (e.g., normal distribution with zero mean and covariance matrix $\mathbf{C}_x$, i.e., $p(\mathbf{x}) \alpha \exp(-\mathbf{x}^T\mathbf{C}_x^{-1}\mathbf{x})$) and obtain a MAP estimator [8]:

$$\hat{\mathbf{x}} = \left(\mathbf{H}^T\mathbf{H} + \sigma_w^2\mathbf{C}_x^{-1}\right)^{-1}\mathbf{H}^T\mathbf{y} = \mathbf{W}\mathbf{y} \qquad (3)$$

Eq. 3 is also known as the Wiener Filtering (WF) deconvolution and has been used for improving the resolution of ultrasound NDE data. WF provides a moderate resolution improvement since the solution is still a smeared version of the MRF [1].

More recently, a new class deconvolution methods exploiting the sparsity of the MRF have emerged in the compressed sensing field [5]. The sparsity is a powerful and natural assumption in ultrasound NDE since there exist a limited number of resolvable echoes along the propagation path. That is, the majority of the elements in MRF ($\mathbf{x}$) are expected to be zero. The sparsity assumption is typically enforced by solving an optimization problem of the form:

$$\hat{\mathbf{x}} = \arg\min\left\{\left\|\mathbf{y} - \mathbf{H}\mathbf{x}\right\|_2^2 + \lambda\left\|\mathbf{x}\right\|_1\right\} \qquad (4)$$

where $\|.\|_n$ denotes the ℓ_n-norm, and $\lambda > 0$ is a regularization parameter controlling the sparsity of the solution. The above optimization problem is convex, hence the optimal solution can be obtained via iterative solvers. In this study, we adopted the ℓ1-ls solver for its simplicity [9]. The MRF obtained via (4) is quite distinct from that of the WF (3) due to the sparsity enforcing ℓ1-norm term in (4). As such this sparse deconvolution technique offers marked resolution improvement and accuracy compared to the WF based methods. However, it assumes the pulse is known and invariant across the measurement. To incorporate pulse variance in sparse deconvolution, one has to model the ultrasound pulse change with varying depth and develop a time-varying attenuation model, i.e., $\mathbf{H} = \mathbf{H}(t)$. Such modeling is not trivial since frequency dependent absorption and scattering characteristics of materials may not be known a priori or may deviate from any assumed model.

We offer an alternative approach to the deconvolution problem by respecting the pulse variance in the RF model (1). The pulse *h(t)* in (1) is too generic such that additional assumptions are required to regularize the pulse shape. An effective regularization approach is to assume a parametric form, i.e.,

$$h_m(t) = h(\boldsymbol{\theta}_m; t) \qquad (5)$$

where $h(\boldsymbol{\theta}; t)$ denotes the pulse model described by a set of parameters stacked in vector $\boldsymbol{\theta}$. With this assumption, the pulse varies according to a pre-specified model. Further, the dimension of $\boldsymbol{\theta}$ is intended to be much smaller than that of $\mathbf{h}$ to achieve a compressed representation of the pulse. With these assumptions, the measurement model (1) is expressed as a superposition of M varying pulses of parametric form (5) in noise, i.e.,

$$y(t_n) = \sum_{m=1}^{M}\beta_m h(t_n - \tau_m; \boldsymbol{\theta}_m) + w(t_n), \;\; n = 0,1,2,...N-1 \qquad (6)$$

Upon (6), the recovery problem is delegated into the estimation of the pulse-shape parameters $\boldsymbol{\theta}_m$ and the MRF parameters $\{\tau_m, \beta_m : m = 1, 2, ..., M\}$ [6]. The measurement model (6) is natural for RF measurement and inherently sparse since the number of echoes is much smaller than the data length, $M << N$. However, the recovery problem in (6) faces two major challenges.

First challenge relates to the choice of a suitable parametric form for transducer pulse *h*. It is well known that the impulse response of an ultrasonic transducer is bandpass with its spectrum concentrated around a center frequency and covers a certain bandwidth. Gaussian Chirplet (GC) model is well suited for such signal representation and has been extensively used for acoustic and ultrasound signal analysis [7]. It provides a reasonable approximation to an echo measured from a point or surface reflector. GC is a Gaussian modulated sinusoid with linear frequency drift. It has 6 parameters: bandwidth factor α, center frequency f_c, chirp rate γ and phase ϕ, along with temporal parameters time-of-arrival (TOA) and amplitude. A unit amplitude GC at TOA 0 is defined as;

$$h(\boldsymbol{\theta}; t_k) = \exp(-\alpha t_k^2)\cos(2\pi f_c t_k + \gamma t_k^2 + \phi), \;\; k = 0,1,..K-1 \qquad (7)$$

where the parameter vector $\boldsymbol{\theta} = [\alpha \; f_c \; \gamma \; \phi]$ contains spectral parameters controlling the shape of the echo.

Second major challenge is the simultaneous estimation of the reflectivity and pulse parameters from the data. This is a multi-dimensional optimization problem and requires an iterative search with respect to all unknown parameters. Such a problem is feasible for a few echoes [1,2] but intractable for a problem of moderate size ($M > 10$). To deal with such an abstract problem, suboptimal reconstruction approaches involving "successive echo estimation and removal from RF data" have been employed [6]. These techniques consists of three major operations: data partitioning based on the assumed echo model (e.g., GC), echo estimation subject to partitioned data, and removal of the estimated echo from the data. This method uses the MAP estimation principle to incorporate a priori belief on the spectral parameters of the pulse thereby controlling the variance of the echo. The computational steps of the algorithm are given in detail in [6].

III. PERFORMANCE EVALUATION VIA COMPUTER SIMULATIONS

We performed restoration of the RF lines by computer simulations to test the performance of the three different algorithms, WF, ℓ1-LSD, and the proposed MBEP. The RF data are generated with a sampling rate of 50 MHz and data length (N) of 1024. Zero-mean white Gaussian noise with variance σ^2=0.0001 is added to the RF line to simulate measurement noise. The amplitude level of the RF line is varied in range $[-1\ \ 1]$. The RF line is created by means of generating a sparse MRF $\mathbf{x}$ of size N with known amplitude and TOA parameters, e.g., $\{\tau_m, \beta_m : m = 1, 2, ..., M\}$, and then assigning echoes of varying shape to each spike located at τ_m with amplitude β_m. The TOA parameters $\{\tau_m, m = 1, 2, ..M\}$ are generated sequentially according to a Poisson distribution, $p(k;\nu) = \frac{\nu^k e^{-\nu}}{k!}$, $k = 0, 1, 2, 3...$ where the parameter ν denotes the mean and variance of the distribution. If the first spike is located at τ_1 (random time index in the beginning of the data trace) then the next spike is placed at $\tau_1 + \Delta\tau$ where $\Delta\tau$ is a random variable drawn from the Poisson distribution with mean ν. The parameter ν is chosen as a fraction of the average pulse length L, e.g., $0.3L$. Once the location of spike is set, the amplitude of the spike is drawn from a zero-mean Laplacian distribution, $p(x;\sigma) = \frac{1}{2\sigma}\exp\left(-\frac{|x|}{\sigma}\right)$ with standard deviation parameter set as $\sigma = 0.5$. A typical MRF generated according to this procedure is shown in Figure 1b in which the spacing between the consecutive spikes vary in range from 10 to 35 with an average spacing of 20. Meanwhile, the varying pulse is generated according to the GC model whose parameter vector $\boldsymbol{\theta}$ (the spectral parameters) is drawn from the normal distribution $N(\boldsymbol{\mu}_\theta, \mathbf{C}_\theta)$ in which the mean parameter vector is assigned to $\boldsymbol{\mu}_\theta = [18(\text{MHz})^2 \quad 0.0 \quad 4.75\text{MHz} \quad 0.5\pi]$ and the covariance matrix $\mathbf{C}_\theta$ is assigned to a [4x4] diagonal matrix, i.e., $diag(\mathbf{C}_\theta) = [2.0 \quad 0.1 \quad 0.2 \quad 2\pi]$. The mean GC echo and 10 different realizations generated according to the normal distribution $N(\boldsymbol{\mu}_\theta, \mathbf{C}_\theta)$ are shown in Figure 1a. One can appreciate that there is perceivable variation among the pulses in terms of their center frequency, bandwidth, and phase.

Using the above RF simulation procedure, based on the MRF shown in Figure 1b and realizations of the GC pulse (10 of them are shown in Figure 1a), a realization of an RF line is shown in Figure 2a. The SNR of this realization is about 25 dB. This RF line was reconstructed using the WF (3), the ℓ1-LSD and MBEP algorithms. For WF and ℓ1-LSD, the mean pulse as shown in Figure 1a was used to construct the degradation matrix $\mathbf{H}$. For WF, the reflectivity variance was set to 0.5. Under these settings, Figure 2b shows the WF restoration along with the actual MRF used in the simulation. The WF provides an attenuated and blurred response which is not sparse. Next, *ℓ1-LSD* algorithm was used to reconstruct this RF line by solving the optimization problem stated in (4). As there are numerous solvers available for this problem, we adopted the ℓ1-ls solver for its simplicity [10]. Using this procedure, Figure 2c shows the *ℓ1-LSD* restoration where the estimated MRF is clearly sparse. However, *ℓ1-LSD* approximates a spike in MRF typically by several spikes. For example, the first spike at time index 30 is represented by five spikes by the *ℓ1-LSD* (see Figure 2c between time indexes 0 and 50). This is because ℓ1-LSD approximates the varying pulse (the echo between time indexes 0 and 50 in Figure 2a) in terms of a number of fixed pulses (Figure 2c).

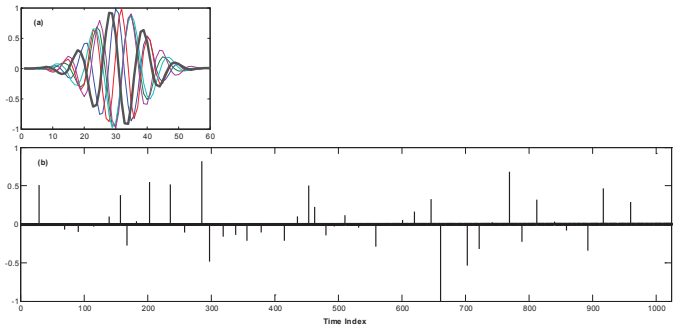

Fig. 1. Simulation of the varying pulse-echo wavelet and the MRF: a) The mean pulse (thick dark line) and 10 different realizations (in colors) generated according to the a priori mean and covariance of the GC parameter vector.
b) A realization of a tissue reflectivity function whose consecutive time-instances and amplitudes are drawn from the Poisson and Laplacian distributions respectively.

For MBEP restoration, the following parameters were used. Analysis window length (used in echo partitioning) was set to the average pulse length L. The prior mean vector was set as $\boldsymbol{\mu}_\theta = [16(MHz)^2 \quad 0.0 \quad 4.5MHz \quad 0.0]$ according to the spectral characteristics (bandwidth and center frequency) of the hypothetical transducer. The chirp rate was set to zero since there will be a minimal drift in frequency in short pulse duration. The phase was set to zero arbitrarily since this parameter is allowed to vary in its full range. To allow variations from the mean pulse, the prior covariance was constructed as $diag(\mathbf{C}_\theta) = [2.0 \quad 0.1 \quad 0.2 \quad 2\pi]$. Meanwhile, the minimum amplitude threshold was set to 0.001, the same as that used in *ℓ1-LSD*. Using these parameters, the MBEP restoration is shown in Fig. 2d along with the original MRF used in the simulation. This restoration is seen to be closest to the actual MRF. It provides a sparser solution than the *ℓ1-LSD* and the individual spikes are generally estimated with high accuracy despite randomly varying pulse in the measurement.

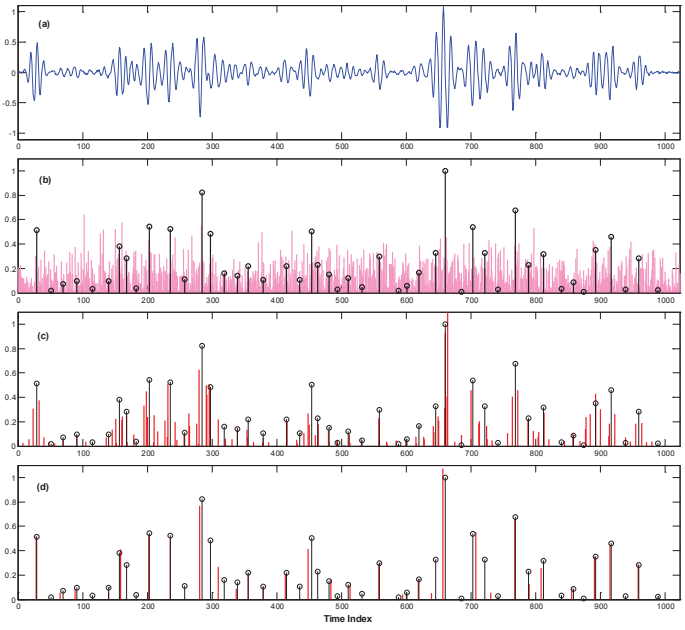

Fig. 2. MRF estimation with different restoration algorithms:
a) The simulated RF line with varying pulse,
b) WF result (red bars) with the actual TRF (dark lines with circles),
c) ℓ1-LSD result (red bars) with the actual TRF,
d) MBEP result (red bars) with the actual TRF.

In order to quantitatively evaluate the performance of the algorithms in recovering the MRF, we used a performance metric, the Correlation Match Index (CMI) defined as,

$$CMI = \frac{\max(\mathbf{r}_{x\hat{x}}) - \mathrm{mean}(\mathbf{r}'_{x\hat{x}})}{\max(\mathbf{r}_{x\hat{x}})} \qquad (8)$$

where $\mathbf{r}_{x\hat{x}}$ denotes the cross-correlation vector between the actual MRF $\mathbf{x}$ and the estimated MRF $\hat{\mathbf{x}}$, and $\mathbf{r}'_{x\hat{x}}$ denotes the cross-correlation vector with the zero-lag element removed. The cross-correlation vector is calculated for a maximum of 10 lags (about 1/4th of the pulse length L) to consider matches within the half-pulse length only. The CMI is a measure of distance between the peak and average value of the cross-correlation and varies between 0 and 1. High values of CMI indicate a good match between the actual and estimated MRFs.

In order to assess and compare the performance of the algorithms in recovering the MRFs, the above RF signal simulation procedure was repeated 100 times. The CMIs and elapsed processing times are calculated and recorded each time. The average values of the CMI and elapsed times are listed in Table 1. It is evident that MBEP provides a higher fidelity restoration of the MRF and is significantly faster than *ℓ1-LSD* and even slightly faster than the WF.

Table 1. Averaged performance metric and processing times of the restoration algorithms for 100 simulated RF lines (SNR is about 25 dB).

	WD	***ℓ1-LSD***	**MBEP**
CMI	0.27	0.70	0.89
Process Time [s] (N=1024)	0.68	9.65	0.56

IV. CONCLUSIONS

In this paper, we modeled the NDE RF signal as a sequence of parametric model echoes whose time-of-arrival and amplitude parameters represent the reflectivity of the scatterers and spectral parameters, which represents the locally varying pulse. These parameters are concurrently estimated from the RF data utilizing the MBEP technique. Through computer simulations, it is shown that the proposed method has a number of advantages compared to a state-of-the-art sparse deconvolution algorithm (*ℓ1-LSD*). First, it is highly flexible with the varying pulse shape. Second, it provides a high fidelity restoration of the MRF. Compared to the *ℓ1-LSD*, the method provides about 25% improvement in restoration fidelity and is about 7 times faster for a typical size data. Although the results are encouraging, further research is warranted to adapt and utilize the technique for the restoration of real ultrasound NDE data.

REFERENCES

[1] R. Demirli, J. Saniie, "Model-Based Estimation of Ultrasonic Echoes, part I: Analysis and algorithms", *IEEE Transactions on Ultrasonics, Ferroelectrics, and Frequency Control (UFFC)*, vol. 48, no. 3, pp. 787-802, May 2001.

[2] R. Demirli and J. Saniie, "Model-based estimation of ultrasonic echoes. Part II: Nondestructive evaluation applications," *IEEE Trans. Ultrasonics, Ferroelectrics and Frequency Control,* vol. 48, no. 3, pp. 803-811, May 2001.

[3] R. Demirli and J. Saniie, "Asymmetric Gaussian chirplet model and parameter estimation for generalized echo representation," *Journal of the Franklin Institute,* vol. 351, no. 2, pp. 907-921, Feb 2014.

[4] G. Cardoso and J. Saniie, "Ultrasonic data compression via parameter estimation," *IEEE Trans. Ultrasonics, Ferroelectrics and Frequency Control,* vol. 52, no. 2, pp. 313-325, Feb 2005.

[5] M. Alessandrini, S. Maggio, J. Poree, L. De Marchi, N. Speciale, O. Bernard and O. Basset, "A restoration framework for ultrasonic tissue characterization," *IEEE Trans.. UFFC,,* vol. 58, , pp. 2344-2360, 2011.

[6] R. Demirli and J. Saniie, " Model-based estimation pursuit for sparse decomposition of ultrasonic echoes," *Signal Processing, IET,* vol. 6, no. 4, pp. 313-325, 2012.

[7] Y. Lu, R. Demirli, G. Cardoso and J. Saniie, " A successive parameter estimation algorithm for chirplet signal decomposition," *IEEE Transactions on UFFC,* vol. 53, no. 11, pp. 2121-2131, 2006.

[8] S. M. Kay, Fundamentals of Statistical Signal Processing, Volume I: Estimation Theory, Upper Saddle River: Prentice Hall, 1994.

[9] S.-J. Kim, K. Koh, M. Lustig, S. Boyd and D. Gorinevsky, "An Interior-Point Method for Large-Scale l1-Regularized Least Squares," *IEEE Journal of Selected Topics in Signal Processing,* vol. 1, no. 4, pp. 606-617, 2007.

[10] K. Koh, S. Kim and S. Boyd, "l1_ls: A Matlab solver for large scale l1-regularized least squares problems," Stanford University, March 2007.